 Human Molecular Genetics, 2002, Vol. 11, No. 12 1455–1464

Systemic and neurologic abnormalities distinguish the lysosomal disorders sialidosis and galactosialidosis in mice

Natalie de Geest, Erik Bonten, Linda Mann, Jean de Sousa-Hitzler, Christopher Hahn† and Alessandra d'Azzo*

Department of Genetics, St Jude Children's Research Hospital, Memphis, TN 38105, USA

Received February 18, 2002; Revised and Accepted March 27, 2002

Neuraminidase initiates the hydrolysis of sialo-glycoconjugates by removing their terminal sialic acid residues. In humans, primary or secondary deficiency of this enzyme leads to two clinically similar neurodegenerative lysosomal storage disorders: sialidosis and galactosialidosis (GS). Mice nullizygous at the *Neu1* locus develop clinical abnormalities reminiscent of early-onset sialidosis in children, including severe nephropathy, progressive edema, splenomegaly, kyphosis and urinary excretion of sialylated oligosaccharides. Although the sialidosis mouse model shares clinical and histopathological features with GS mice and GS patients, we have identified phenotypic abnormalities that seem specific for sialidosis mice. These include progressive deformity of the spine, high incidence of premature death, age-related extramedullary hematopoiesis, and lack of early degeneration of cerebellar Purkinje cells. The differences and similarities identified in these sialidosis and GS mice may help to better understand the pathophysiology of these diseases in children and to identify more targeted therapies for each of these diseases.

INTRODUCTION

Neuraminidases/sialidases (EC 3.2.1.18) comprise a superfamily of hydrolytic enzymes that have a conserved active site and similar sequence motifs. In vertebrates, neuraminidases perform an indispensable role in the catabolism of sialic acid-containing glycoconjugates and, like sialic acids, have been implicated in crucial biological processes, from cell proliferation/differentiation and cell adhesion, to clearance of plasma proteins, catabolism of gangliosides and glycoproteins, and modification of receptors (1–3). The pivotal function of these enzymes may account for the existence of three mammalian neuraminidases encoded by different genes and defined as lysosomal, cytosolic and plasma-membrane on the basis of their subcellular distribution, pH optimum, kinetic properties and substrate specificity (4–11). Lysosomal neuraminidase is ubiquitously expressed in various tissues and cell types, and functions exclusively in a multienzyme complex containing at least two other hydrolases, the glycosidase β-galactosidase and the carboxypeptidase protective protein/cathepsin A (PPCA). Its association with PPCA is essential for the correct transport of the enzyme to the lysosome and catalytic activation (12,13).

Defective or deficient lysosomal neuraminidase activity is associated with two neurodegenerative disorders of glycoprotein metabolism: sialidosis (mucolipidosis I), caused by structural lesions in the lysosomal neuraminidase gene, and galactosialidosis (GS), a combined deficiency of lysosomal neuraminidase and β-galactosidase that is due to the absence of functional PPCA. Patients with sialidosis and those with GS have similar clinical and biochemical features that are likely attributable to the absence of neuraminidase function. Different clinical variants exist in both diseases, differing in the age of onset and severity of the symptoms (14,15). Type I or cherry-red spot/myoclonus syndrome (16,17) is a late-onset non-dysmorphic form of sialidosis. Patients suffer from intention myoclonus and progressive visual failure, and have only minimal intellectual impairment (18). Type II sialidosis presents with abnormal somatic features, skeletal dysplasia, hepatosplenomagaly and moderate/severe mental retardation. The juvenile/infantile subtypes of type II sialidosis are relatively normal at birth, but develop progressive visceromegaly, dysostosis multiplex and mental retardation; they usually survive to the second decade of life, and may develop cherry-red spots and myoclonus (19). Nephrosialidosis is considered a variant of the infantile form, with features of mucopolysaccharidosis and a

*To whom correspondence should be addressed at: Department of Genetics, St Jude Children's Research Hospital, 332 North Lauderdale, Memphis, TN 38105, USA. Tel: + 1901 495 2698; Fax: + 1901 526 2907; Email: sandra.dazzo@stjude.org
†Present address: Christopher Hahn, Vascular Biology Laboratory, Hanson Centre for Cancer Research, Adelaide, Australia 5000

glomerulopathy with increasing proteinuria (20–23). Widespread neuronal and systemic lysosomal storage, particularly in the kidney, are the main characteristics. The congenital form of sialidosis is associated with hydrops fetalis and/or neonatal ascites with stillbirth or early death (24,25). Facial edema, inguinal hernia, hepatosplenomegaly, stippling of the epiphyses and periosteal cloaking may be present at birth. These severe early-onset forms are clinically similar to the early infantile forms of GS (15). The percentage of residual neuraminidase activity in sialidosis patients' tissues and cultured cells mostly depends on the type of mutation in the NEU1 gene, and correlates inversely with the clinical severity (12).

We have generated PPCA$^{-/-}$ mice that develop pathological manifestations reminiscent of GS patients (26), including progressive nephropathy, severe ataxia and shortened lifespan. A partial deficiency of neuraminidase has occurred spontaneously in the mouse strain SM/J (27) and is associated with a Leu295Ile amino acid substitution in the neuraminidase protein (28). However, the residual enzyme activity in these mice is too high to provoke a sialidosis phenotype. We have now generated a mouse line that is completely devoid of lysosomal neuraminidase. From a comparative analysis of these mice and the GS mice, we could identify phenotypic differences that suggest distinct roles for neuraminidase and cathepsin A activities in specific physiological pathways.

RESULTS

Biochemical features of Neu1$^{-/-}$ mice are diagnostic of sialidosis

Homozygous null mice lacked all four Neu1 transcripts (Fig. 1C), and had severely reduced neuraminidase activity in most tissues tested compared with Neu1$^{+/+}$ littermates; heterozygotes had intermediate enzyme values (Fig. 2A, upper panel). A relatively high residual activity was measured in muscle, thymus and brain, likely due to the plasma-membrane and cytosolic neuraminidases, which are unaffected in these mice, and are well expressed in these tissues (8). Figure 2A shows the average enzyme values measured in tissue homogenates from four different Neu1$^{-/-}$ mice of the NMRI colony at the age of 3 weeks. In spite of the presence of the other two neuraminidases in some tissues, the amounts of the lysosomal enzyme in Neu1$^{+/+}$ tissues seems to correlate with the levels of Neu1 mRNA detected on northern blots, with the highest activity being found in kidney and intestine, and the lowest in spleen, heart and lung. In contrast, the activity of the bacterial β-galactosidase marker (LacZ, expressed by the targeted Neu1 locus) in kidney, spleen and intestine paralleled that of lysosomal neuraminidase in the corresponding wild-type tissues (Fig. 2A, B), but was significantly higher in liver, lung and heart, raising the possibility that a feedback mechanism may upregulate the Neu1 promoter in absence of neuraminidase.

Young mutant mice (1–2 months) already had a prominent oligosaccharidiuria, which is diagnostic of the disease in children with either sialidosis or GS. The oligosaccharide pattern was similar to that detected in age-matched PPCA$^{-/-}$ mice, linking this biochemical defect to the severeneuraminidase deficiency in both mouse models (Fig. 2C). At a late stage of the disease (∼8 months and older), Neu1$^{-/-}$ mice had mild hypoproteinemia: total protein, 3.6 g/100 ml (normal range 4.4–6.2); globulin, 1.3 g/100 ml (1.9–3.2); albumin, 2.3 g/100 ml (2.6–4.6). Glucose content was occasionally lower in animals older than 7 months (111 mg/dl) (normal range 124–262), although at this age mutant mice become passive and fed poorly, which could, in turn, affect the glucose levels in the blood.

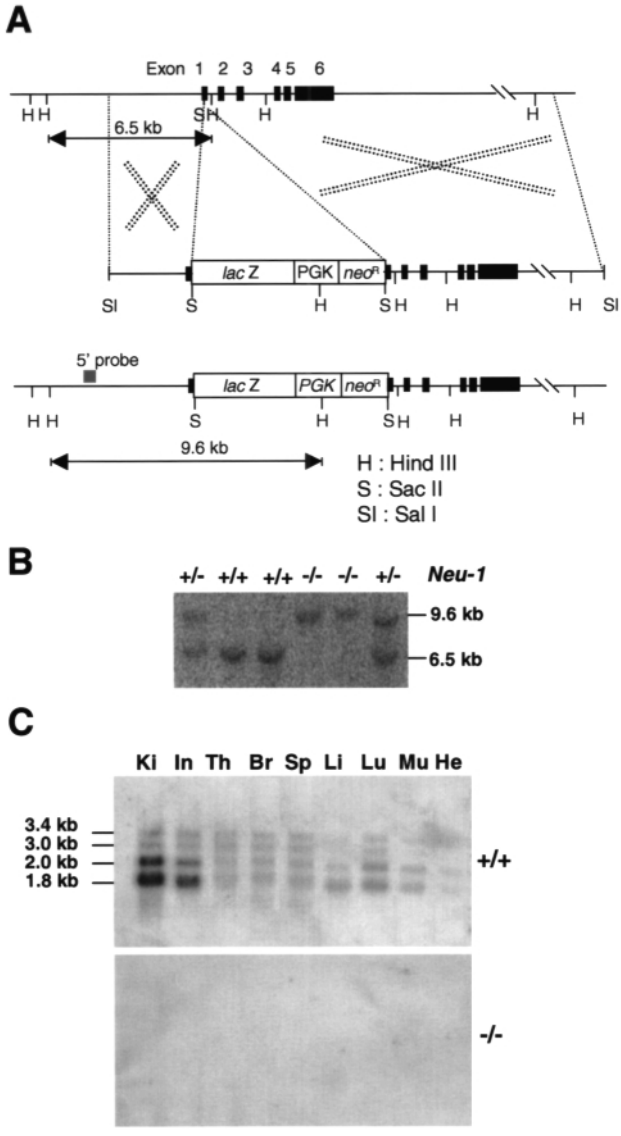

Figure 1. Generation of Neu1$^{-/-}$ mice. (A) The structure of the Neu1 gene, the targeting construct and the predicted structure of the disrupted Neu1 locus after homologous recombination are represented schematically. Only relevant restriction sites are shown. The numbered solid boxes are exons. The 5′ probe (gray box) used for screening of the targeted clones detects a 9.6 kb HindIII fragment derived from the mutant allele and a 6.5 kb HindIII fragment derived from the wild-type allele. (B) Southern blot analysis of HindIII-digested genomic DNA, isolated from F_2 mouse tails and probed with the 5′ probe depicted in (A). Two Neu1 homozygous null mice are distinguished by the presence of only the diagnostic 9.6 kb fragment. (C) Northern blot analysis of poly(A)$^+$ RNA from various tissues of 8-week-old Neu1$^{-/-}$ and Neu1$^{+/+}$ mouse, probed with the full-length 1.8 kb neuraminidase cDNA demonstrate the absence in the mutant mouse of the four Neu1 transcripts detected in the wild-type mouse.

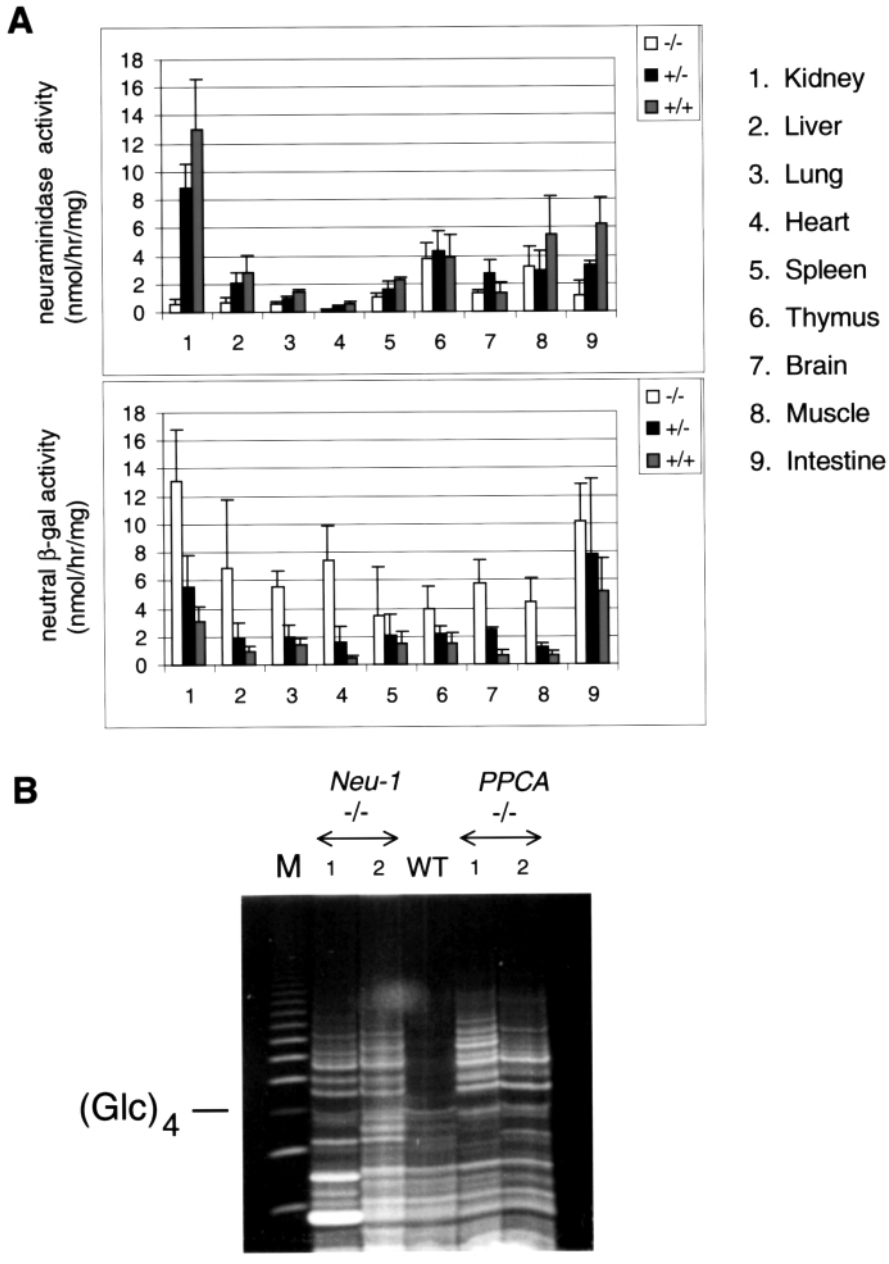

Figure 2. Biochemical analysis of Neu1$^{-/-}$ mice. (A) Comparison of the neuraminidase and β-galactosidase activities measured in various tissues of wild-type (Neu1$^{+/+}$), heterozygous (Neu1$^{+/-}$) and knockout (Neu1$^{-/-}$) mice of 3 weeks of age. Averages were made from the results of 4 animals. (B) Carbohydrate profiles in urine samples of 1-month-old (lanes 1) and 2-month-old (lanes 2) Neu1$^{-/-}$ and PPCA$^{+/-}$ mice, compared to a 2-month-old wild-type control. Deficient mice show increased urinary excretion of high-molecular-weight oligosaccharides (oligosaccharide markers are shown in lane M).

Electrolytes (sodium, potassium, and calcium), creatinine and blood urea nitrogen (BUN) values were within normal limits.

As observed in patients with sialidosis or GS (29), peripheral blood smears from affected mice of various ages showed prominent vacuolation in practically all lymphocytes, monocytes and eosinophils, but not in neutrophils (not shown).

Clinical phenotype

In the two genetic backgrounds, newborn Neu1$^{-/-}$ mice weighed about 25% less than their heterozygous or wild-type littermates (Fig. 3A). This feature was consistent with PPCA mutant mice. However, 27% of the Neu1$^{-/-}$ pups in the NMRI background and 10–15% in the C57BL/6 background died suddenly around weaning age – a feature not seen in the GS model. Hyperkeratosis of the stomach suggested that the cause of death was inanition after 1–2 days of anorexia. Mice that survived past the 21 days were fertile, but stopped producing offspring by the age of 10 weeks. Edema of the subcutaneous tissues, limbs, penis, forehead and eyelids developed already at 4–6 weeks of age, and progressively worsened. Kyphosis of the lumbar spine and lordosis of the cervical and thoracic spine

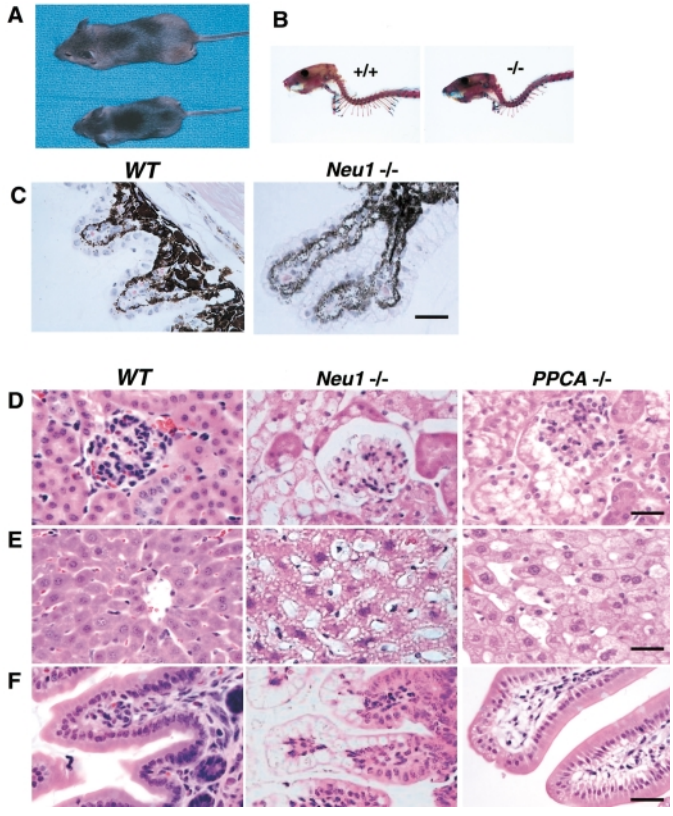

Figure 3. Clinical and histopathological phenotype of Neu1$^{-/-}$ mice. (A) Neu1 null mice are 25% smaller than their wild-type littermates (shown: 1-month-old littermates). (B) Skeletal staining of a 5-month-old Neu1$^{-/-}$ mouse indicates increased curvature of the cervical spine. (C–F) Histopathological analysis of a 5-month-old (C–E) or a 3-week-old (F) Neu1$^{-/-}$ mouse compared with an age-matched PPCA$^{-/-}$ mouse and a wild-type (PPCA$^{+/+}$) littermate. Paraffin sections were stained with H&E. (C) Examination of the eyes of Neu1$^{-/-}$ mice showed ballooned epithelial cells of the ciliary body and conjunctiva. (D) In the kidney, prominent vacuolation is seen in both $-/-$ models in the epithelial cells of the proximal convoluted tubuli and the glomeruli. (E) The liver sections of both mutant mice show severe ballooning of Kupffer cells and microvacuolation of the hepatocytes. (F) The apical epithelial cells of the intestinal villi of a Neu1$^{-/-}$ mouse are excessively vacuolated, potentially leading to deficient nutrient absorption and anorexia. This feature is not detected in age-matched PPCA$^{-/-}$ mice. Size bars: 25 μm (C–E); 50 μm (F).

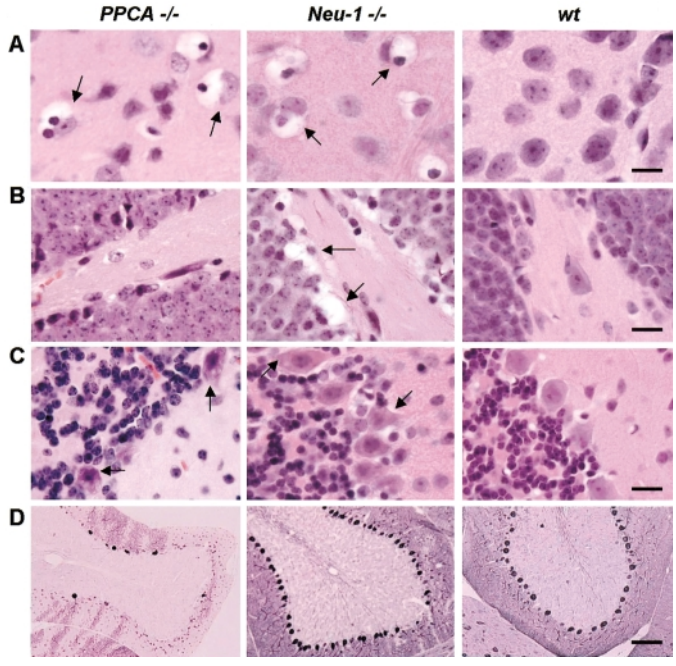

Figure 4. Brain pathology of a 5-month-old Neu1$^{-/-}$ mouse compared with an age-matched PPCA$^{-/-}$ mouse and a wild-type littermate ($+/+$). (A) As in GS mice, microglia and perivascular macrophages throughout the brain parenchyma (arrowheads) are generally filled with storage (shown is the nucleus putamen). (B) The dendate gyrus is often more severely affected in the Neu1$^{-/-}$ mouse (arrowheads) than in the PPCA$^{-/-}$ mouse. (C) In contrast to the extensive loss of the Purkinje cells in the PPCA$^{-/-}$ cerebellum (arrowheads indicate vaculated Purkinje cells), no or very little degeneration is visible in Neu1$^{-/-}$ cerebellum (arrowheads indicate Purkinje cells with few or no vacuoles). (A–C) H&E staining. (D) Low-magnification image of a cerebellar lobe shows a dramatic difference in the total number of Purkinje cells in the PPCA$^{-/-}$ mouse compared with the Neu1$^{-/-}$ mouse of the same age. These sections were immunostained with an antibody against the PEP19 marker. Size bars: 20 μm (A–C); 100 μm (D).

became prominent by the age of 6 months, although skeletal analysis revealed only an enhanced curvature of the cervical vertebrae (Fig. 3B). A shock-like twitch indicative of peripheral nervous system involvement was a consistent phenotype in mutant mice. At the end of their lifespan they appeared weak and debilitated, and suffered from dyspnea, loss of weight, gait abnormalities, and tremor. Death occurred between the ages of 8 and 12 months.

Pathology of Neu1$^{-/-}$ mice reveals systemic lysosomal storage diseases comparable to GS mice

For histopathology, Neu1$^{-/-}$ mice were sacrificed at 1, 2, 5 and 8 months of age and compared with age-matched PPCA$^{-/-}$ mice (26,30). Light microscopy of H&E-stained tissues showed extensive vacuolation of some cells in most of the systemic organs. In particular, the kidney was the earliest and most affected organ – a feature also characteristic of GS mice (Fig. 3D, PPCA$^{-/-}$) and typical of sialidosis and GS patients. Proximal more than distal and collecting tubules were extensively vacuolated already at 1 month of age. At 3 months, also the epithelial cells of the glomeruli and the Bowman capsule were affected (Fig. 3D, Neu1$^{-/-}$). In the liver, primarily Kupffer cells appeared ballooned, although with age sinusoidal cells and hepatocytes also became filled with vacuoles (Fig. 3E, Neu1$^{-/-}$ and PPCA$^{-/-}$). Despite the high expression of lysosomal neuraminidase in the wild-type intestine, overt abnormalities in the gastrointestinal tract were not evident in the adult mutant mice (not shown). However, autopsy on the $-/-$ pups that had succumbed suddenly at weaning revealed that the epithelial cells of the villi were markedly dilated with large, apical vacuoles. This feature, which was consistently present in Neu1$^{-/-}$ pups, was clearly less severe in GS mice (Fig. 3F, Neu1$^{-/-}$ and PPCA$^{-/-}$).

Although all Neu1$^{-/-}$ mice showed severely distended bladder and urinary retention starting at the age of 6 months, there were no clear morphological changes in the urethral epithelium. However, the mice suffered from hydronephrosis, evidenced by enlarged kidneys with a markedly dilated renal pelvis. Inconspicuous lysosomal storage was detected in the

heart, skeletal muscle and lung, with the exception of the endothelial cells lining the capillaries (not shown). Examination of the eyes showed that cytoplasmic vacuolation was restricted to the epithelial cells of the ciliary body and the conjunctiva (Fig. 3C). The latter was strikingly similar to what has been observed in a sialidosis patient (31).

Neu1$^{-/-}$ mice developed a pattern of disease in the brain similar but not identical to that in GS mice. Extensive storage was apparent in the epithelial cells of the choroid plexi and in the endothelial cells of the ependymal layer. Although vacuolated neurons were sparsely detected throughout the parenchyma (primarily in the olfactory bulb, the subolfactory nucleus and the nuclei of the limbic system), microglia and perivascular macrophages were generally the most affected cells, and were often seen juxtaposed to degenerating neurons (Fig. 4A, Neu1$^{-/-}$ and PPCA$^{-/-}$). Numerous ballooned macrophage-like cells appeared to line neurons of the dentate gyrus only in the Neu1$^{-/-}$ mice (Fig. 4B, Neu1$^{-/-}$). One of the most overt abnormalities seen in the brain of GS mice is the progressive loss of Purkinje cells starting at 2–3 months of age and resulting in ataxic movements and lack of coordination (26,32). These cells die sequentially in an antero-posterior, medio-lateral fashion, the anterior lobes being the ones that are affected most and sooner. A comparative numeric and spatial analysis of the Purkinje cells in 5-month-old Neu1$^{-/-}$ and PPCA$^{-/-}$ animals demonstrated that the cerebellar lobes that showed more than 90% cell loss in the PPCA$^{-/-}$ (Fig. 4C, D PPCA$^{-/-}$) mice were not significantly affected in the Neu1$^{-/-}$ mice (Fig. 4C, D, Neu1$^{-/-}$). This was seen in both genetic backgrounds.

Extramedullary hematopoiesis as the cause of splenomegaly in Neu1$^{-/-}$ mice

In contrast to the PPCA$^{-/-}$ mice, enlargement of the spleen was consistently observed in Neu1$^{-/-}$ mice, starting at 6 weeks of age; the spleen size increased steadily to reach a maximum at 5–6 months, but normalized again later in life (Fig. 5A). This increase in size was accompanied by a progressive increase on total cell counts up to 5 months that decreased thereafter (Fig. 5B, spleen); instead, cell counts in total bone marrow (BM) were lower than in wild-type mice (Fig. 5B, BM). In histological sections, the BM cavity was filled with numerous ballooned macrophages (Fig. 5D), although the BM did not show any marked changes in the hematopoietic profiles, as assessed by flow cytometry, using hematopoietic markers for progenitors (CD117/c-Kit) or myeloid (Mac-1, Gr-1), erythroid (Ter119) and lymphoid (B220, CD3, CD4, CD8, Sca-1, Thy1.2) (not

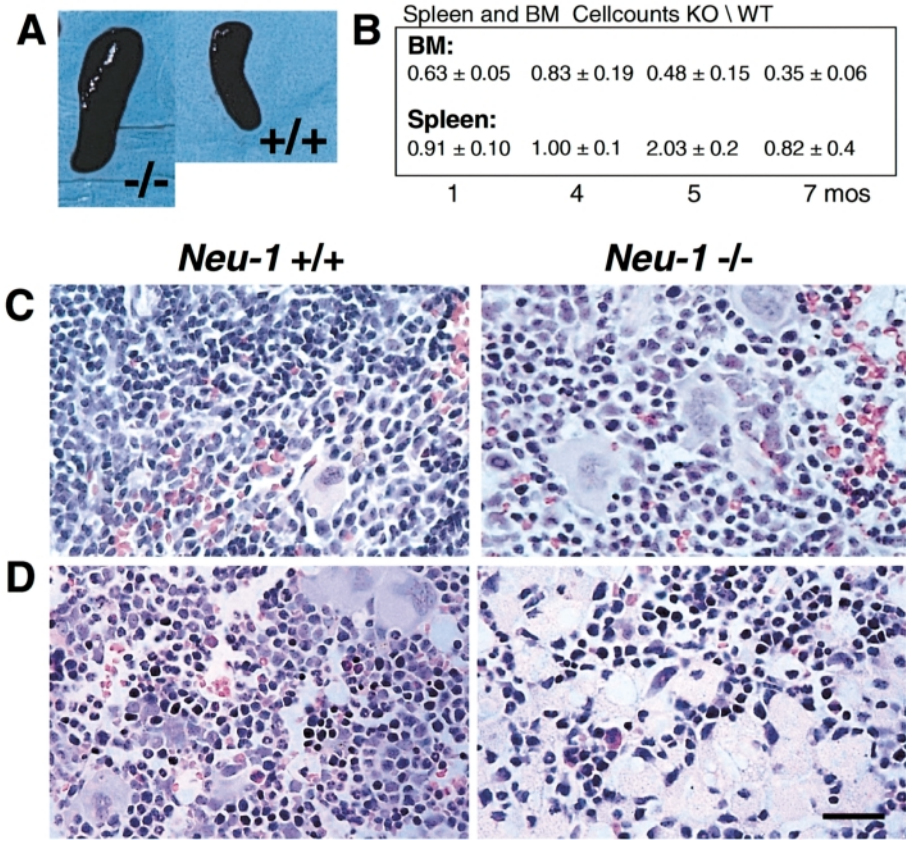

Figure 5. The spleen of Neu1$^{-/-}$ mice is a major site of extramedullary hematopoiesis. (A) Spleens of 5-month-old Neu1$^{-/-}$ mice are 3-fold larger than spleens from wild-type littermates. (B) Cell-count ratios for spleen and bone marrow (8 m) of Neu1$^{-/-}$ animals compared with control animals at different age-points demonstrate increased cellularity in the spleen, and a slight decreased cellularity in the BM at the 5-month time point. Paraffin sections of spleen (C) and decalcified bone (D) from Neu1$^{-/-}$ and Neu1$^{+/+}$ mice, stained with H E, show increased number of splenic megakaryocytes and massive infiltration of macrophages in the BM of deficient animals. Size bars: 25 μm (C,D).

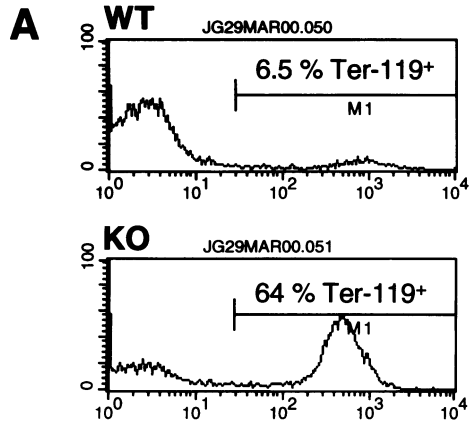

%Ter119+ KO/WT

BM:				
	1.07 ± 0.10	0.99 ± 0.10	1.15 ± 0.20	0.86 ± 0.10
Spleen:				
	1.78 ± 0.4	5.29 ± 1.5	4.14 ± 1.0	2.72 ± 1.1
	1	4	5	7 mos

B

		Spleen Methocult Counts				BM Methocult Counts			
BFU	WT	31 ± 5	4 ± 1	0 ± 0	13 ± 1	9 ± 3	2 ± 0	4 ± 1	8 ± 1
	KO	25 ± 5	29 ± 6	2 ± 0	27 ± 16	10 ± 2	1 ± 0	4 ± 1	7 ± 2
GM	WT	34 ± 7	20 ± 4	3 ± 1	35 ± 5	20 ± 2	28 ± 2	14 ± 1	28 ± 1
	KO	33 ± 7	29 ± 6	7 ± 2	54 ± 10	18 ± 3	33 ± 3	12 ± 2	26 ± 6
GEMM	WT	13 ± 4	7 ± 2	9 ± 3	16 ± 5	7 ± 1	5 ± 2	25 ± 3	5 ± 2
	KO	11 ± 3	12 ± 2	17 ± 5	25 ± 10	7 ± 1	5 ± 1	25 ± 2	7 ± 2
TOTAL	WT	79 ± 2	31 ± 5	12 ± 2	63 ± 8	36 ± 3	34 ± 3	43 ± 3	42 ± 3
	KO	70 ± 9	70 ± 17	25 ± 3	106 ± 33	34 ± 2	39 ± 3	40 ± 4	41 ± 9
months		1	4	5	7	1	4	5	7

Figure 6. (A) Increased number of erythroid progenitor cells in spleen and bone marrow (8 m) of Neu1$^{-/-}$ versus Neu1$^{+/+}$ mice as measured by FACS analysis of spleen and BM cell suspensions marked with anti-Ter119 antibody. The two left panels represent an example of histograms from a 5-month-old Neu1$^{-/-}$ (KO) and a Neu1$^{+/+}$ (WT) mouse, showing a 10-fold increment in the number of Ter119-positive cells. (B) Methylcellulose colony-forming assays on spleen and BM cell suspensions from Neu1$^{-/-}$ versus Neu1$^{+/+}$ mice. The increased number of clonogenic precursors in mutant spleen peeks at the age of 5 months.

shown) lineages. However, an increased number of megakaryocytes were visible in H&E-stained sections of the spleen (Fig. 5C). Flow cytometry of splenic cell suspensions incubated with anti-Ter119 demonstrated a 2–10-fold increase in the number of erythroid precursors (Fig. 6A). This feature was not evident in Neu1$^{-/-}$ BM. Combined, these data were indicative of extramedullary hematopoiesis (EMH) as the cause of splenic hypertrophy in Neu1$^{-/-}$ mice. To ascertain whether the changes in cell numbers reflected differences in the differentiation or distribution of hematopoietic progenitors, the number of lineage-committed progenitors was determined in Neu1$^{-/-}$ mice between 1 and 7 months of age, using methylcellulose colony-forming assays. The number of clonogenic precursors in the BM was comparable to that of wild-type mice, regardless of age. Instead all clonogenic precursors were increased in the spleen (Fig. 6B): erythroid burst-forming units (BFU-E) 5-fold in 4-month-old mice and 2-fold in 7-month-old mice; granulocyte–macrophage and granulocyte–erythroid–macrophage–megakaryocyte colony forming units (CFU-GM and CFU-GEMM) 2-fold at all time-points. Immunohistochemical analysis of mutant livers with anti-Ter119 antibody showed a high number of erythroblasts, indicative of extramedullary hematopoiesis in this organ as well. However, this phenomenon became prominent only at about 7 months of age (not shown).

DISCUSSION

Molecular and biochemical features of Neu1$^{-/-}$ mice correlate well with the severe dysmorphic form of human sialidosis. Although viable, mutant mice present signs of illness early in life with evidence of lysosomal storage in virtually all organs, affecting primarily epithelial, (reticulo)endothelial and histiocytic (monocytic/phagocytic macrophages) cells. Most of the pathological changes seen in the Neu1$^{-/-}$ mice resemble closely those of the GS mouse model (26,30), reinforcing the notion that the loss of neuraminidase activity in both mutants is the primary cause of the disease. On close observation, however, we have identified differences that could eventually help to distinguish the function of cathepsin A and neuraminidase in the expression of the phenotype.

Like patients with sialidosis and GS, Neu1$^{-/-}$ mice have growth impairment and remain smaller than their healthy littermates throughout their lifespan. This feature is also characteristic of the PPCA$^{-/-}$ and SM/J mouse models (26,27,30), but is accompanied in the Neu1 mutants by a high incidence of sudden death. Although we do not know the molecular basis of this phenomenon, we hypothesize that it could be caused by the significant and abrupt increase in the turnover of epithelial cells in the small intestine of suckling pups (11–14

days) compared with that in mice right after weaning (2 days) (33). This would explain why the intestine is much more affected in the Neu1$^{-/-}$ pups than in the Neu1$^{-/-}$ weaned mice, and why the apical cells of the villi are more ballooned than the cells of the crypts. The extensive vacuolation of the apical epithelial cells could interfere mechanically with normal nutrient absorption, or cause a decreased formation and recycling of normal absorptive vacuoles. This pathology could lead to starvation during lactation, and explain the decreased size of homozygous null mice and the sudden-death phenotype at 3 weeks of age by inanition. Although not fully penetrant, this phenotype is clearly specific for Neu1$^{-/-}$ mice and is not seen in PPCA$^{-/-}$ mice, suggesting a primary role for lysosomal neuraminidase in the maintenance of intestinal cell homeostasis during the postnatal period. It is possible that increased survival through the critical 2–3 weeks period could be obtained by dietary supplementation of easily absorbed nutrients, since dietary changes are known to be critical in modifying the epithelial mucin predominately in the small intestine (34).

Although only minor bone changes have been identified in mutant mice, it is still possible that impaired function of osteoclasts causes inefficient bone remodeling which may contribute to their small size (35). This hypothesis could be in keeping with observed bone deformities in children with nephrosialidosis and type II sialidosis (20,23).

The pronounced vacuolation of renal tubular and glomerular epithelium in Neu1$^{-/-}$ mice correlates with the high expression of neuraminidase in kidney, and is characteristic of human sialisodis and GS. Inefficient renal filtration is accompanied by proteinuria and diffuse edema, as indeed are observed in the mutant mice early in life. Although hypoproteinemia and/or proteinuria is reported in all nephrosialidosis patients, loss of protein into the serum was only detected in some of the mice and was never accompanied by electrolyte imbalance. A similar discrepancy has been reported for an infantile sialidosis patient with severe edema, swollen glomerular and tubular epithelial cells of the kidney, without evidence of renal involvement (36). It is unclear whether the penetrance of this phenotype in patients mirrors the severity of the neuraminidase mutation(s), which may affect differently the cellular distribution of the mutant protein and/or the type and extent of accumulated products. In addition, other genetic factors that alone are not causing disease, when combined with a neuraminidase deficiency may predispose to or provoke renal dysfunction.

Neu1$^{-/-}$ mice develop a pronounced but transient splenomegaly characterized by an increased number of megakaryocytes and red blood cell precursors, and elevated numbers of hematopoietic precursors. These features are characteristic of EMH. Splenic EMH can occur as a secondary response to (i) failure of BM hematopoiesis (37–39), (ii) anemia (e.g. following hemorrhage), (iii) bacterial infection (40,41) or (iv) myelofibrosis (41). We have no evidence supporting the latter three in triggering EMH in our mutant mice. However, we did observe a reduction in the total number of BM cells recovered from the hindlegs of Neu1$^{-/-}$ mice, suggesting that impaired BM hematopoiesis could cause mobilization of BM-derived progenitors to the spleen. EMH could simply be the result of crowding of the BM cavities by ballooned cells, or could have a more complex physiological cause, such as impaired bone remodeling. These hypotheses, however, do not explain the strict age dependence of this phenomenon. It is noteworthy that similar age-related changes have been observed in CSF-1 mutant and osteopetrosis mice (op/op), where occlusion of the BM cavities is caused by excessive bone formation (38,39,43). Also in these cases, however, it is unclear why EMH disappears in older mice. Another physiological cause of EMH in the sialidosis model could relate to a potential role of lysosomal neuraminidase in providing the optimal microenvironment for the homing of BM cells, for example by participating in the processing of adhesion molecules, integrins or growth factors (or their receptors) at their cell surface (44), similarly to what has been reported for the cytosolic enzyme (45).

The neurologic phenotype of Neu1$^{-/-}$ mice is similar to that of the GS model and is reminiscent of other mouse models of lysosomal disorders [e.g. Niemann-Pick A and B (46,47) and Sanfilippo B (48)], where microglia and perivascular macrophages more than neurons are the primary target of the disease. The characteristic pattern of Purkinje cell death in GS mice, however, is not observed in the Neu1$^{-/-}$ mutants. Given the severe deficiency of neuraminidase secondary to the loss of PPCA in the GS model, one would have predicted a nearly identical phenotype. An intriguing observation is that while PPCA is highly expressed in normal Purkinje cells, neuraminidase is not, suggesting that the death of these cells in GS mice cannot be attributed to the secondary neuraminidase deficiency, but instead may be the result of the loss of cathepsin A catalytic activity. We still have little understanding of the physiological role of cathepsin A activity outside the complex and in different cell types, which could involve ancillary pathways. If this is the case, then this phenotypic abnormality may represent the first evidence that loss of cathepsin A activity may cause disease. This hypothesis could be tested experimentally by creating a PPCA mutant mouse expressing a protein that has lost its catalytic activity but retains its protective function towards neuraminidase and β-galactosidase (49).

The availability of mouse models of both sialidosis and GS will facilitate comparative studies of the pathogenesis of these diseases in children as well as the development of targeted therapies for each of these diseases.

MATERIALS AND METHODS

Gene targeting in ES cells and generation of homozygous null mice

The mouse Neu1 gene was cloned from a 129/Sv embryonic stem (ES) cell genomic library (28,30). A 10 kb SalI fragment encompassing all six exons (Fig. 1A) was used to generate the targeting vector. A *β*-geo cassette with the LacZ reporter gene and the Neo-selectable marker driven by the PGK promoter (LacZ/PGK/neo) was inserted in frame into a unique SacII site within exon 1. Homologous recombination at the Neu1 locus would result in the transcription of the LacZ gene from the Neu1 endogenous promoter, and in the translation of a neuraminidase protein truncated after the 33 amino acids of the signal peptide.

W9.5 ES cells were grown on irradiated mouse embryonic fibroblasts (MEFs) feeders and electroporated as described

previously (26). The ES cells were allowed to recover for 24 h, after which they were cultured in the presence of 350 μg/ml G418 (BioWittaker) for 7 days. Resistant ES clones were screened for homologous recombination of the targeted allele by Southern blotting of HindIII-digested genomic DNA, using a 600 bp BamHI/EcoRI probe located immediately upstream of the targeted region (Fig. 1A). Correctly targeted clones were identified by the presence of a diagnostic 9.6 kb fragment in addition to the normal 6.5 kb band (Fig. 1B). Positive clones were karyotyped. The absence of additional random integrations of the construct was verified on Southern blots containing genomic DNA digested with EcoRI, which cut inside the *β*-geo cassette and released a diagnostic fragment of 8.5 kb, followed by hybridization with a Neo probe (not shown). Targeted ES cells were microinjected into C57BL/6 blastocysts at the SJCRH Transgenic Core Facility. Neu1 heterozygous mice were interbred to homozygosity for assessment of the phenotype and backcrossed to C57B1/6 and NMRI lines to determine the influence of the genetic background on disease expression. Litters were genotyped by Southern blotting (Fig. 1B). Null mice were obtained in both genetic backgrounds at a frequency of 23% (expected 25% $-/-$, 25% $+/+$ and 50% $+/-$), indicating the absence of perinatal death (Fig 1B). The PPCA$^{-/-}$ mice used in comparative studies are in a C57B1/6 background.

Northern blotting

Total RNA was isolated from different tissues, collected from 3- to 8-week old mice, using Trizol Reagent (Invitrogen); poly(A)$^{+}$ RNA was purified with the Oligotex mRNA kit (Qiagen). Poly-(A)$^{+}$ RNA (3 μg) was separated on 1% agarose gels containing 0.66 M formaldehyde, blotted onto Zeta-probe membranes (Bio-Rad) and hybridized in Express Hyb (Clontech) with a ^{32}P-labeled mouse full-length neuraminidase cDNA probe (1.8 kb).

Histopathological studies

Mice were perfused transcardially with 0.1 M sodium phosphate, pH 7.4/4% paraformaldehyde. Dissected organs were either processed for paraffin embedding or frozen in tissue freezing medium (Triangle Biomedical Sciences, Durham, NC) after 24–48 h incubation in 30% sucrose/0.1 M sodium phosphate, pH 7.4. Paraffin sections were routinely stained with hematoxylin/eosin (H&E), using standard procedures. Staining of the skeletons was performed as described in (50). Cerebellar slides were also immunostained with an antibody against the PEP19 marker (51) (a kind gift of Dr J. Morgan, Developmental Neurobiology, SJCRH).

Enzyme assays and urinary oligosaccharide analysis

Tissues from euthanized, non-perfused Neu1$^{-/-}$ and wild-type mice in both C57B1/6 and NMRI backgrounds were homogenized on ice in 4 volumes (w/v) of milli-Q water (Millipore), using a 2 ml Wheaton tissue grinder. The activities of neuraminidase (pH 4.3) and neutral β-galactosidase (pH 7.0) were assayed with artificial 4-methylumbelliferylneuraminic acid and 4-methylumbelliferyl-β-galactoside substrates (Sigma), respectively (52). Total protein concentrations of tissue homogenates were determined using the BCA assay (Pierce). Urinary complex carbohydrates were resolved on high-resolution polyacrylamide gels and visualized by fluorophore-assisted carbohydrate electrophoresis (FACE) according to the manufacturers' protocol (Glyko, Novato, CA).

Hematologic and chemical analyses

Serum and urine samples from Neu1$^{-/-}$ and wild-type mice were analyzed for total protein, albumin, globulin, sodium, potassium, calcium, glucose, BUN and creatinine content by Ani-Lytics Inc. (Gaithersburg, MD). Hematological counts were performed on heparinized blood collected by eye bleed with an EDTA-coated capillary using standard procedures (Laboratory of Analysis of the Animal Resource Center at SJCRH).

Hematopoietic progenitor cell assay

Spleen, femur and tibia specimens were dissected from Neu1$^{-/-}$ and wild-type mice at 1, 3, 5 and 7 months of age. BM was flushed from the femur and tibia in 10 ml Iscove's medium, supplemented with 10% fetal bovine serum, using a syringe and 25-gauge needle. Single-cell suspensions were obtained by passing spleen and BM through cell strainers. Cell viability and density were determined by trypan blue staining after lysis of red blood cells in 1% acetic acid (v/v). Methylcellulose cultures for the analysis of clonogenic precursors were prepared according to the manufacturer's protocol (M3434, StemCell Technologies Inc.). After 12 days' incubation (humidified 5% CO_2), BFU-E, GM-CFU, and GEMM-CFU were counted in duplicate dishes (30 mm diameter), each containing at least 50 colonies.

Flow cytometry

Cell suspensions from spleen or BM (2×10^6 cells/ml) were incubated for 30 min at 4°C with fluorophore-conjugated antibodies against various hematopoietic markers. The one relevant for these studies, PE anti-Ter119 (Pharmingen), was used at a 5–20 μg/ml concentration in PBS, 1% BSA, followed by a wash step with PBS, 10% BSA (v/w). FACS analysis was performed on a FACS-Calibur cytometer (Becton Dickinson, San Jose, CA), acquiring 5000–10 000 events. FACS data were analyzed using CellQuest software.

ACKNOWLEDGEMENTS

We are grateful to Dr Gerard Grosveld for his continuous support, to Christie Nagy and John Raucci (Transgenic Core Facility, SJCRH) for blastocyst injections, to Dr Robbert Rottier for providing the mouse neuraminidase gene, to Dr Charles Clifford (Charles River Laboratory) for expert pathology, to Dr Huimin Hu for his assistance in making the histology figures, to James Knowles for help in maintaining the mouse colonies and in genotyping, and to Charlette Hill for help in editing the manuscript. This work was supported by grants from the National Institutes of Health (DK52025 and GM60950), the Assisi Foundation of Memphis, the Cancer

Center Support Grant CA 21765, and the American Lebanese Syrian Associated Charities (ALSAC) of St Jude Children's Research Hospital.

REFERENCES

1. Schauer, R., Kelm, S., Reuter, G., Roggentin, P. and Shaw, L. (1995) Biochemistry and role of sialic acids. In Rosenberg, A. (ed.), Biology of the Sialic Acids. Plenum Press, New York, pp. 7–67.
2. Saito, M., Tanaka, Y., Tang, C., Yu, R. and Ando, S. (1995) Characterization of sialidase activity in mouse synaptic plasma membranes and its age-related changes. J. Neurosci. Res., 40, 401–406.
3. Reuter, G. and Gabius, H.-J. (1996) Review: Sialic acids: structure–analysis–metabolism–occurrence–recognition. Biol. Chem. Hoppe Seyler, 377, 325–342.
4. Bonten, E.J. and d'Azzo, A. (2000) Lysosomal neuraminidase. Catalytic activation in insect cells is controlled by the protective protein/cathepsin A. J. Biol. Chem., 275, 37657–37663.
5. Bonten, E., Spoel, A.v.d., Fornerod, M., Grosveld, G. and d'Azzo, A. (1996) Characterization of human lysosomal neuraminidase defines the molecular basis of the metabolic storage disorder sialidosis. Genes Dev., 10, 3156–3169.
6. Miyagi, T., Konno, K., Emori, Y., Kawasaki, H., Suzuki, K., Yasui, A. and Tsuiki, S. (1993) Molecular cloning and expression of cDNA encoding rat skeletal muscle cytosolic sialidase. J. Biol. Chem., 268, 26435–26440.
7. Ferrari, J., Harris, R. and Warner, T.G. (1994) Cloning and expression of a soluble sialidase from Chinese hamster ovary cells: sequence alignment similarities to bacterial sialidases. Glycobiology, 4, 367–373.
8. Miyagi, T., Wada, T., Iwamatsu, A., Hata, K., Yoshikawa, Y., Tokuyama, S. and Sawada, M. (1999) Molecular cloning and characterization of a plasma membrane-associated sialidase specific for gangliosides. J. Biol. Chem., 274, 5004–5011.
9. Wada, T., Yoshikawa, Y., Tokuyama, S., Kuwabara, M., Akita, H. and Miyagi, T. (1999) Cloning, expression, and chromosomal mapping of a human ganglioside sialidase. Biochem. Biophys. Res. Commun., 261, 21–27.
10. Monti, E., Preti , A., Rossi, E., Ballabio, A. and Borsani, G. (1999) Cloning and characterization of NEU2, a human gene homologous to rodent soluble sialidases. Genomics, 57, 137–143.
11. Fronda, C.L., Zeng, G., Gao, L. and Yu, R.K. (1999) Molecular cloning and expression of mouse brain sialidase. Biochem. Biophys. Res. Commun., 258, 727–731.
12. Bonten, E.J., Arts, W.F., Beck, M., Covanis, A., Donati, M.A., Parini, R., Zammarchi, E. and d'Azzo, A. (2000) Novel mutations in lysosomal neuraminidase identify functional domains and determine clinical severity in sialidosis. Hum. Mol. Genet., 9, 2715–2725.
13. van der Spoel, A., Bonten, E. and d'Azzo, A. (1998) Transport of human lysosomal neuraminidase to mature lysosomes requires protective protein/cathepsin A. EMBO J., 17, 1588–1597.
14. Thomas, C.E., Schiedner, G., Kochanek, S., Castro, M.G. and Lowenstein, P.R. (2001) Preexisting antiadenoviral immunity is not a barrier to efficient and stable transduction of the brain, mediated by novel high-capacity adenovirus vectors. Hum. Gene Ther., 12, 839–846.
15. d'Azzo, A., Andria, G., Strisciuglio, P. and Galjaard, H. (2001) Galactosialidosis. In Scriver, C., Beaudet, A., Sly, W. and Valle, D. (eds), The Metabolic and Molecular Bases of Inherited Disease. 8th edn. McGraw-Hill, New York, 3, pp. 3811–3826.
16. Durand, P., Gatti, R., Cavalieri, S., Borrone, C., Tondeur, M., Michalski, J.C. and Strecker, G. (1977) Sialidosis (mucolipidosis I). Helv. Paediatr. Acta, 32, 391–400.
17. Rapin, I., Goldfischer, S., Katzman, R., Engel, J., Jr, and O'Brien, J.S. (1978) The cherry-red spot–myoclonus syndrome. Ann. Neurol., 3, 234–242.
18. Thomas, G.H. (2001) Disorders of glycoprotein degradation and structure: α-mannosidosis, β-mannosidosis, fucosidosis, and sialidosis. In Scriver, C.R., Beaudet, A.L., Sly, W.S. and Valle, D. (eds), The Metabolic and Molecular Bases of Inherited Disease, 8th edn. McGraw-Hill, New York, 3, pp. 3507–3534.
19. Young, I.D., Young, E.P., Mossman, J., Fielder, A.R. and Moore, J.R. (1987) Neuraminidase deficiency: case report and review of the phenotype. J. Med. Genet., 24, 283–290.
20. Maroteaux, P., Humbel, R., Strecker, G., Michalski, J.C. and Mande, R. (1978) A new type of sialidosis with kidney disease: nephrosialidosis. I. Clinical, radiological and nosological study [in French]. Arch. Fr. Pediatr., 35, 819–829.
21. Le Sec, G., Stanescu, R. and Lyon, G. (1978) A new type of sialidosis with kidney disease: nephrosialidosis. II. Anatomic study [in French]. Arch. Fr. Pediatr., 35, 830–844.
22. Aylsworth, A., Thomas, G., Hood, J., Malouf, N. and Libert, J. (1980) A severe infantile sialidosis: clinical biochemical and microscopic features. J. Pediatr., 96, 662–668.
23. Kelly, T.E., Bartoshesky, L., Harris, D.J., McCauley, R.G., Feingold, M. and Schott, G. (1981) Mucolipidosis I (acid neuraminidase deficiency). Three cases and delineation of the variability of the phenotype. Am. J. Dis. Child., 135, 703–708.
24. Riches, W.G. and Smuckler, E.A. (1983) A severe infantile mucolipidosis. Clinical, biochemical, and pathologic features. Arch. Pathol. Lab. Med., 107, 147–152.
25. Beck, M., Bender, S.W., Reiter, H.L., Otto, W., Bassler, R., Dancygier, H. and Gehler, J. (1984) Neuraminidase deficiency presenting as non-immune hydrops fetalis. Eur. J. Pediatr., 143, 135–139.
26. Zhou, X.Y., Morreau, H., Rottier, R., Davis, D., Bonten, E., Gillemans, N., Wenger, D., Grosveld, F.G., Doherty, P., Suzuki, K. et al. (1995) Mouse model for the lysosomal disorder galactosialidosis and correction of the phenotype with overexpressing erythroid precursor cells. Genes Dev., 9, 2623–2634.
27. Potier, M., Yan, D. and Womack, J. (1979) Neuraminidase deficiency in the mouse. FEBS Lett., 108, 345–348.
28. Rottier, R., Bonten, E. and d'Azzo, A. (1998) A point mutation in the neu-1 locus causes the neuraminidase defect in the SM/J mouse. Hum. Mol. Genet., 7, 313–321.
29. Zammarchi, E., Donati, M.A., Marrone, A., Donzelli, G., Zhou, X.Y. and d'Azzo, A. (1996) Early infantile galactosialidosis: clinical, biochemical, and molecular observations in a new patient. Am. J. Med. Genet., 64, 453–458.
30. Rottier, R., Hahn, C., Mann, L., Martin, M., Smeyne, R., Suzuki, K. and d'Azzo, A. (1998) Lack of PPCA expression does not always correlate with lysosomal storage: a possible requirement for the catalytic function of PPCA in galactosialidosis. Hum. Mol. Gen., 7, 1787–1794.
31. Matsuo, T., Egawa, I., Okada, S., Suhtsugui, M., Yamamoto, K. and Watanabe, M. (1983) Sialidosis type 2 in Japan. Clinical study in two siblings cases and review of literature. J. Neurol. Sci., 58, 45–55.
32. Hahn, C., Martin, M., Zhou, X., Mann, L. and d'Azzo, A. (1998) Correction of murine galactosialidosis by bone marrow-derived macrophages overexpressing human protective protein/cathepsin A under control of the colony-stimulating factor-1 receptor promoter. Proc. Natl Acad. Sci. USA, 95, 14880–14885.
33. Bertram, T. (1991) Gastrointestinal Tract. Academic Press, San Diego.
34. Sharma, R., Schumacher, U. (2001) Carbohydrate expression in the intestinal mucosa. Adv. Anat. Embryol. Cell Biol., 160, 1–91.
35. Teitelbaum, S.L. (2000) Bone resorption by osteoclasts. Science, 289, 1504–1508.
36. Yamano, T., Shimada, M., Matsuzaki, K., Matsumoto, Y., Yoshihara, W., Okada, S., Inui, K., Yutaka, T. and Yabuuchi, H. (1986) Pathological study on a severe sialidosis (alpha-neuraminidase deficiency). Acta Neuropathol. (Berl.), 71, 278–284.
37. Deguchi, K., Yagi, H., Inada, M., Yoshizaki, K., Kishimoto, T. and Komori, T. (1999) Excessive extramedullary hematopoiesis in Cbfa1-deficient mice with a congenital lack of bone marrow. Biochem. Biophys. Res. Commun., 255, 352–359.
38. Nilsson, S.K. and Bertoncello, I. (1994) Age-related changes in extramedullary hematopoiesis in the spleen of normal and perturbed osteopetrotic (op/op) mice. Exp. Hematol., 22, 377–383.
39. Begg, S.K. and Bertoncello, I. (1993) The hematopoietic deficiencies in osteopetrotic (op/op) mice are not permanent, but progressively correct with age. Exp. Hematol., 21, 493–495.
40. Lai, Y.H., Heslan, J.M., Poppema, S., Elliot, J.F. and Mosmann, T.R. (1996) Continuous administration of Il-13 to mice induces extramedullary hemopoiesis and monocytosis. J. Immunol., 156, 3166–3173.
41. Staber, F.G. and Metcalf, D. (1980) Cellular and molecular basis of the increased splenic hemopoiesis in mice treated with bacterial cell wall components. Proc. Natl Acad. Sci. USA, 77, 4322–4325.
42. Weinstein, I.M. (1991) Idiopathic myelofibrosis: historical review, diagnosis and management. Blood Rev., 5, 98–104.

43. Begg, S.K., Radley, J.M., Pollard, J.W., Chisholm, O.T., Stanley, E.R. and Bertoncello, I. (1993) Delayed hematopoietic development in osteopetrotic (op/op) mice. J. Exp. Med., 177, 237–242.
44. Muller-Sieburg, C.E. and Deryugina, E. (1995) The stromal cells' guide to the stem cell universe. Stem Cells, 13, 477–486.
45. Sawada, M., Moriya, S., Saito, S., Shineha, R., Satomi, S., Yamori, T., Tsuruo, T., Kannagi, R. and Miyagi, T. (2002) Reduced sialidase expression in highly metastatic variants of mouse colon adenocarcinoma 26 and retardation of their metastatic ability by sialidase overexpression. Int. J. Cancer, 97, 180–185.
46. Horinouchi, K., Erlich, S., Perl, D.P., Ferlinz, K., Bisgaier, C.L., Sandoff, K., Desnick, R.J., Stewart, C.L. and Schuchman, E.H. (1995) Acid sphingomyelinase deficient mice: a model of types A and B Niemann–Pick disease. Nat. Genet., 10, 288–293.
47. Otterbach, B. and Stoffel, W. (1995) Acid sphingomyelinase-deficient mice mimic the neurovisceral form of human lysosomal storage disease (Niemann–Pick diseases). Cell, 81, 1053–1061.
48. Li, H.H., Yu, W.H., Rozengurt, N., Zhao, H.Z., Lyons, K.M., Anagnostaras, S., Fanselow, M.S., Suzuki, K., Vanier, M.T. and Neufeld, E.F. (1999) Mouse model of Sanfilippo syndrome type B produced by targeted disruption of the gene encoding alpha-N-acetylglucosaminidase. Proc. Natl Acad. Sci. USA, 96, 14505–14510.
49. Galjart, N.J., Morreau, H., Willemsen, R., Gillemans, N., Bonten, E.J. and d'Azzo, A. (1991) Human lysosomal protective protein has cathepsin A-like activity distinct from its protective function. J. Biol. Chem., 266, 14754–14762.
50. Alkema, M.J., Bronk, M., Verhoeven, E., Otte, A., van't Veer, L.J., Berns, A. and van Lohuizen, M. (1997) Identification of Bmi1-interacting proteins as constituents of a multimeric mammalian polycomb complex. Genes Dev., 11, 226–240.
51. Smeyne, R.J. and Goldowitz, D. (1990) Purkinje cell loss is due to a direct action of the weaver gene in Purkinje cells: evidence from chimeric mice. Brain Res. Dev. Brain. Res., 52, 211–218.
52. Galjaard, H. (1980) Genetic Metabolic Disease: Diagnosis and Prenatal Analysis. Elsevier Science, Amsterdam.